

See discussions, stats, and author profiles for this publication at: <https://www.researchgate.net/publication/264721559>

Structural Properties and the Effect of 2,6-Diaminoanthraquinone on G-Tetrad, Non-G-Tetrads, and Mixed Tetrads—A Density Functional Theory Study

ARTICLE *in* INTERNATIONAL JOURNAL OF QUANTUM CHEMISTRY · OCTOBER 2011

Impact Factor: 1.43 · DOI: 10.1002/qua.22720

CITATIONS

5

READS

10

3 AUTHORS, INCLUDING:



Palanisamy Deepa

Manonmaniam Sundaranar University

21 PUBLICATIONS 65 CITATIONS

SEE PROFILE



K. Senthilkumar

Bharathiar University

78 PUBLICATIONS 1,445 CITATIONS

SEE PROFILE

Structural Properties and the Effect of 2,6-Diaminoanthraquinone on G-Tetrad, Non-G-Tetrads, and Mixed Tetrads—A Density Functional Theory Study

P. DEEPA, P. KOLANDAIVEL, K. SENTHILKUMAR

Department of Physics, Bharathiar University, Coimbatore 641 046, India

Received 7 December 2009; accepted 8 March 2010

Published online 6 October 2010 in Wiley Online Library (wileyonlinelibrary.com).

DOI 10.1002/qua.22720

ABSTRACT: Telomerase inhibitor causes the attrition of telomere length and consequently leading to senescence which require a lag period for cancer cells to stop proliferating. Telomeric sequences form quadruplex structures stabilized by tetrads. The structural and electronic properties related with interaction of 2,6-diaminoanthraquinone and tetrads are the key step to elucidate the anticancer activity. The present study has been focused on the stability of the isolated tetrads and the effect of interaction of 2,6-diaminoanthraquinone with G-tetrad, non-G-tetrads, and mixed tetrads using density functional theory method in both gas and aqueous phases. The solvent interaction with the molecular systems has increased the stability of the isolated tetrads and complexes. The sharing of electron density between the interacting molecules is shown through electron density difference maps. The atoms in molecules theory and natural bond orbital analysis have been performed to study the nature of hydrogen bonds in the inhibitor interacting complexes. The linear correlation is shown between electron density [$\rho(r)$], and its Laplacian [$\nabla^2\rho(r)$] at the bond critical points. The strong binding nature of 2,6-diaminoanthraquinone with studied tetrads reveals that this inhibitor is suitable to stabilize the above tetrads and inhibit the telomerase activity. © 2010 Wiley Periodicals, Inc. *Int J Quantum Chem* 111: 3239–3250, 2011

Key words: telomerase; tetrads; 2,6-diaminoanthraquinone; interaction energy; atoms in molecules; natural bond orbital analysis

Correspondence to: P. Kolandaivel; e-mail: ponkvel@hotmail.com

1. Introduction

Nucleic acid repeat sequences that fold into three-dimensional tetraplex structures have attracted much interest among scientists because of their involvement in many important biological functions and structural characteristics [1–3]. Telomerase is the enzymatic activity that maintains the ends of eukaryotic chromosomes by protecting the chromosome from recombination, end-to-end fusion and nuclease degradation [4–8]. For human beings, telomerase activity is highly regulated by the expression of the human telomerase reverse transcriptase (hTERT) gene. Inhibition or activation of the hTERT expression could profoundly affect the proliferative capacity of normal and cancer cells [9–11]. Because telomerase activity is directly related with proliferation of immortal cells, and cancer cells, it has become the focus of much attention as a potentially specific target for the development of new anticancer chemotherapeutics. The use of cytotoxic agents to kill cancer cells and telomerase inhibitor to limit the proliferative potential of residual cancer cells are the regular procedure in cancer chemotherapy. Telomerase inhibitor causes the attrition of telomere length and consequently leading to senescence, which require a lag period for cancer cells to stop proliferating [12].

In this respect, the molecular inhibitors such as tetra-(*N*-methyl-2-pyridyl)-porphyrins, 2,7-disubstituted fluorenones, 2,6-diaminoanthraquinone (ANTH), and dicationic piperidino perylene tetracarboxylic diamide have demonstrated experimentally for telomerase inhibition activity [12, 13]. The inhibitor 2,6-diaminoanthraquinone (ANTH) stabilizes the folded DNA quadruplex structure with low level of general cytotoxicity [14] and modulates hTERT expression, cell growth, and telomerase inhibition [15–21]. As revealed in several crystal and NMR studies [22] DNA sequences are associated strongly together through inter- and intra-molecular interactions to form a variety of quadruplex structures, including stacked tetrads. The structural uniqueness of G-quadruplex DNA makes it an ideal target for drug design, so the earlier experimental and theoretical studies were focused on quadruplexes containing only GGGG tetrads [23–28]. The crystallographic studies show that GCGC tetrads were found in telomeric DNA [29–34]. Non-G-tetrads and mixed tetrads such as ATGC, ATAT, ATAA, ATTT, GCCC,

and GCGG exhibiting the versatility of quadruplexes have been reported in several crystallographic and NMR studies [35–37].

The structural and electronic properties related with interaction of 2,6-diaminoanthraquinone (ANTH) and DNA tetrads are the key step to elucidate the anticancer activity of 2,6-diaminoanthraquinone. A complete theoretical study on the G, non-G, and mixed tetrads and their 2,6-diaminoanthraquinone interacting complexes is not available in the literature. Hence, the present study is focused on the inhibitor activity of 2,6-diaminoanthraquinone with usual DNA tetrads. The structure and function of DNA is highly sensitive to surrounding water medium [38]. Hence, in the present study, the inhibitor activity of ANTH has been studied in water medium also. The structure, interaction energy, many body interaction energies, and electron density analysis have been used to understand the inhibitor activity of 2,6-diaminoanthraquinone with usual DNA tetrads.

2. Computational Approach

The Becke's three parameter (B3) exchange functional along with the Lee-Yang-Parr's (LYP) gradient corrected correlation functional [39, 40] represented as B3LYP of density functional theory (DFT) method with 6-31G** basis set have been used to optimize G, non-G, and mixed tetrads and their 2,6-diaminoanthraquinone interacting complexes. Vibrational frequency calculations show that all the optimized tetrads and 2,6-diaminoanthraquinone interacting complexes are real minima without imaginary frequencies. Single point energy calculations have been performed to study the solute-solvent interaction using the self-consistent reaction field theory (SCRF)[41] at B3LYP/6-31G** level of theory. This method is based on Tomasi's polarized continuum model (PCM), which defines the cavity as the union of a series of interlocking atomic spheres.

The interaction energies have been corrected for the basis set superposition error (BSSE) using counterpoise correction method [42]. Because the role of individual energy components of interaction energy is important to analyze the active sites of inhibitor and tetrads, the many body analysis [43] have been performed, by partitioning the interaction energy into two and five body interactions,

$$\begin{aligned}\Delta E_{\text{TOTAL}} &= E_{(\text{ABCDE})} - [E_{(\text{A})} + E_{(\text{B})} + E_{(\text{C})} + E_{(\text{D})} \\ &\quad + E_{(\text{E})}] \\ \Delta^5 E(\text{ABCDE}) &= \Delta E_{\text{TOTAL}} - [\Delta^2 E(\text{AB}) + \Delta^2 E(\text{AC}) \\ &\quad + \Delta^2 E(\text{BC}) + \Delta^2 E(\text{AD}) \\ &\quad + \Delta^2 E(\text{AE}) + \Delta^2 E(\text{BD}) \\ &\quad + \Delta^2 E(\text{BE}) + \Delta^2 E(\text{CD}) \\ &\quad + \Delta^2 E(\text{CE}) + \Delta^2 E(\text{DE})] \\ \Delta^2 E(\text{AB}) &= E_{\text{AB}} - [E_{(\text{A})} + E_{(\text{B})}]\end{aligned}$$

where $E_{(\text{ABCDE})}$ is the total energy of inhibitor interacting complexes, E_{A} , E_{B} , E_{C} , E_{D} , and E_{E} are the total energy of single base or inhibitor, and E_{AB} is the total energy of any two interacting molecules (base pairs or base with an inhibitor). The electron density $\rho(r)$ and its second derivative, Laplacian of electron density $\nabla^2 \rho(r)$ for hydrogen bonds using Bader's atoms in molecules (AIM) theory [44–47] has been performed. NBO analysis has been performed to study the charge transfer property in the interacting orbitals [48]. All these calculations have been performed using the Gaussian 03W package [49].

3. Results and Discussion

The optimized structures of G, non-G, and mixed tetrads and their 2,6-diaminoanthraquinone inhibitor interacting complexes have been shown in the Figures 1 and 2. In G-tetrad, the Guanine bases are linked through Hoogsteen pairing or by bifurcated hydrogen bonds between N1-H, N2-H, and O6 atoms as reported in [23–28, 50–52]. Guanine tetrad is formed between the donor and acceptor atoms (see Fig. 1). This structure is in agreement with a quadruplex structure formed in antiparallel DNA sequences [52]. GCGC tetrad consists of two GC pairs linked through hydrogen bonds between H4 of amino group and O6 of the other base pairs as observed by Gu et al. [34] and Meyer et al. [53]. The ATAT tetrad is formed through bifurcated hydrogen bonding between O4 of thymine and the amino group of adenine bases [35, 54]. Each thymine is simultaneously bonded with two adenine bases. It has been shown that the ATAT tetrad is further stabilized by stacking with sugar pucker of the preceding thymine [35, 54]. The ATGC, GCGG, and GCCC tetrads are formed through the bifurcated hydrogen bonding between carbonyl group of guanine, cytosine and thymine

nucleobases with amino group of adenine, guanine, and cytosine bases. The ATAA and ATTT tetrads are formed as Hoogsteen and Watson Crick arrangement and no bifurcated hydrogen bonding is observed between the bases.

The stable tetrads are responsible for the formation of DNA sequences. The existence of planar or near-planar tetrads is of special importance since planar tetrads can be further stabilized by successive tetrads through stacking interactions [55–58]. The tetrads GCCC and GCGC are having planar or near planar structure due to the formation of strong bifurcated hydrogen bonds. The intrinsic pyramidalization of the amino group in nucleobases, electrostatic interactions, and steric hindrance between the base pairs disturb the planarity in ATGC, GCGG, GGGG, ATAT, ATAA, and ATTT tetrads. The binding of inhibitor through hydrogen bond led to a structural change in DNA tetrads around the amine, amide, and keto groups of the nucleobases. As shown in the Figure 2, the inhibitor 2,6-diaminoanthraquinone (ANTH) directly interacts with the amine and keto groups of nucleobases, which increase the steric hindrance between the bases and reduce the planarity in the complexes. The intrinsic non-planarity and structural change in the tetrads can influence the function of DNA [59].

The isolated tetrads and ANTH interacting tetrads are formed through N–H...N and N–H...O type hydrogen bonds. In addition to N–H...N (O) type hydrogen bonds, C–H...O type hydrogen bonds are formed in ATAT-ANTH, ATGC-ANTH, and GCGC-ANTH complexes. The calculated hydrogen bond lengths were presented in Table I and shown in Figure 1. The N–H...N (O) type hydrogen bonds are relatively strong with bond length of 1.76–2.2 Å. The hydrogen bond length of C–H...O interaction is in the range of 1.96–2.5 Å. In isolated tetrads and ANTH interacting complexes, GCGC, GGGG, and GCGC tetrads are having 8–10 hydrogen bonds, whereas ATTT, ATAT, and ATAA tetrads are having 5–7 hydrogen bonds only. Upon the interaction of 2,6-diaminoanthraquinone, the hydrogen bond length within the base pairs and between two base pairs increases by 0.06 Å and 0.1 Å, respectively, and bond angles by 1–4° as shown in Figure 2. The distance between the edges of the minor or major groove of one base pair to other base pair has been taken as the tetrad length. For isolated tetrads, the tetrad length value ranges from 7.8 to 15.6 Å, and for ANTH interacting complexes, the tetrad length

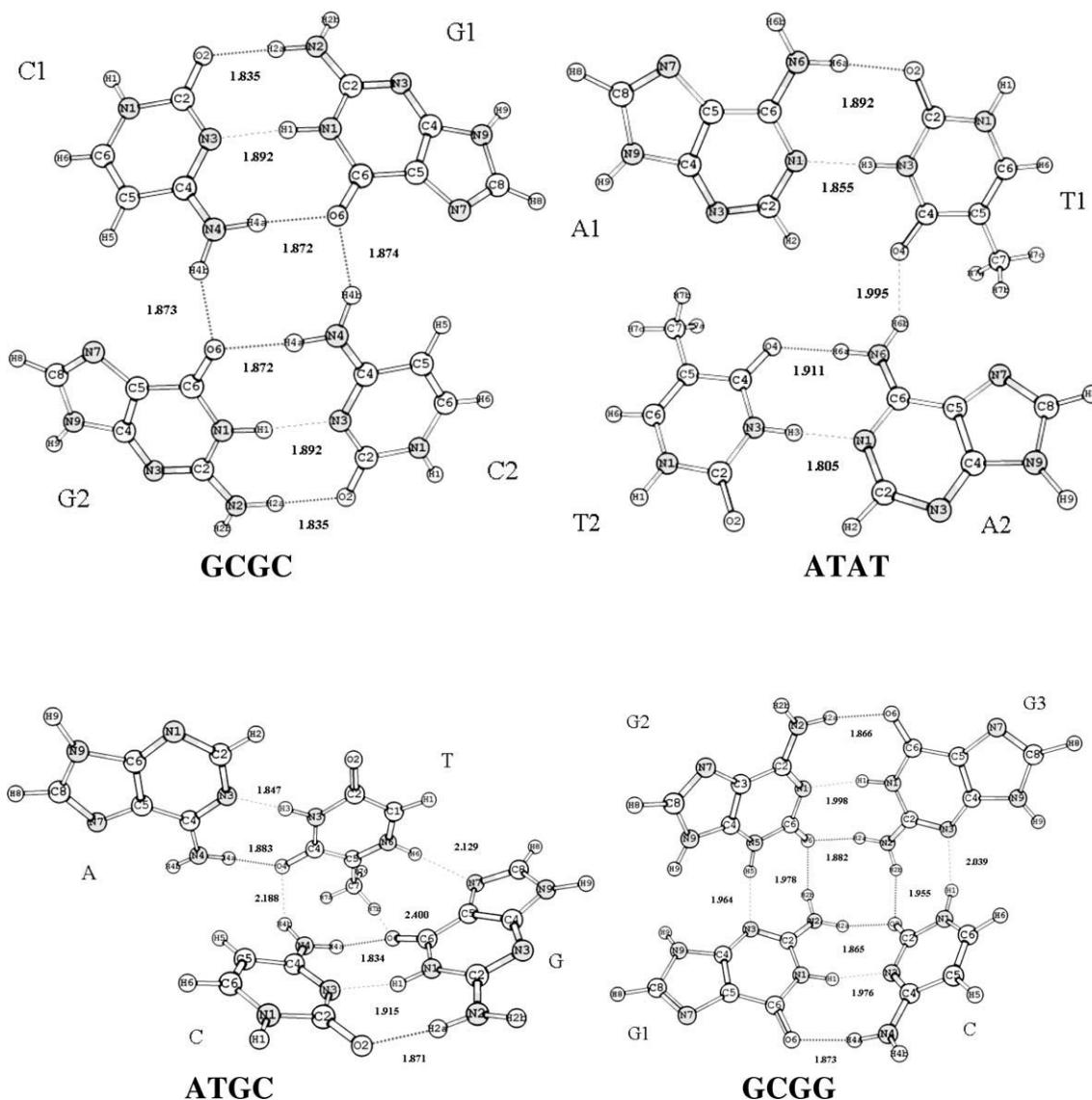


FIGURE 1. The structures of isolated tetrads (GCGC, ATAT, ATGC, GCGG, GCCC, ATAA, and ATTT) optimized at B3LYP/6-31G** level of theory (IUPAC number has been followed for labeling of atoms).

value varies from 8.6 to 12.3 Å. Thus, the interaction of 2,6 diaminoanthraquinone with the tetrad makes the base pair to bend inwards at the minor or major groove edges, which considerably decrease the tetrad length around 2 Å. For ATAT and ATGC tetrads, the tetrad length is slightly increased by 0.12–1.2 Å, respectively, upon the interaction of 2,6-diaminoanthraquinone.

The calculated hydrogen bond interaction energies were corrected for BSSE and are summarized in Table II. The interaction energy calculated for ATAT tetrad is found to be –33.61 kcal/mol, which is comparable with the previous reported

[35] values of –30.43 kcal/mol calculated at B3LYP/6-311G** level of theory. GCGC tetrad has more interaction energy of –81.14 kcal/mol, which is due to the presence of more of number of N–H...O type hydrogen bonds in the structure. As shown in Figure 2, the GCGC and GCCC tetrads are formed with the parallel orientation of base pairs. The ATTT tetrad has relatively less interaction energy of –29.68 kcal/mol with a perpendicular orientation of base pairs. The interaction energy order for isolated tetrads is GCGC > GGGG > GCCC > GCGG > ATGC > ATAA > ATAT > ATTT.

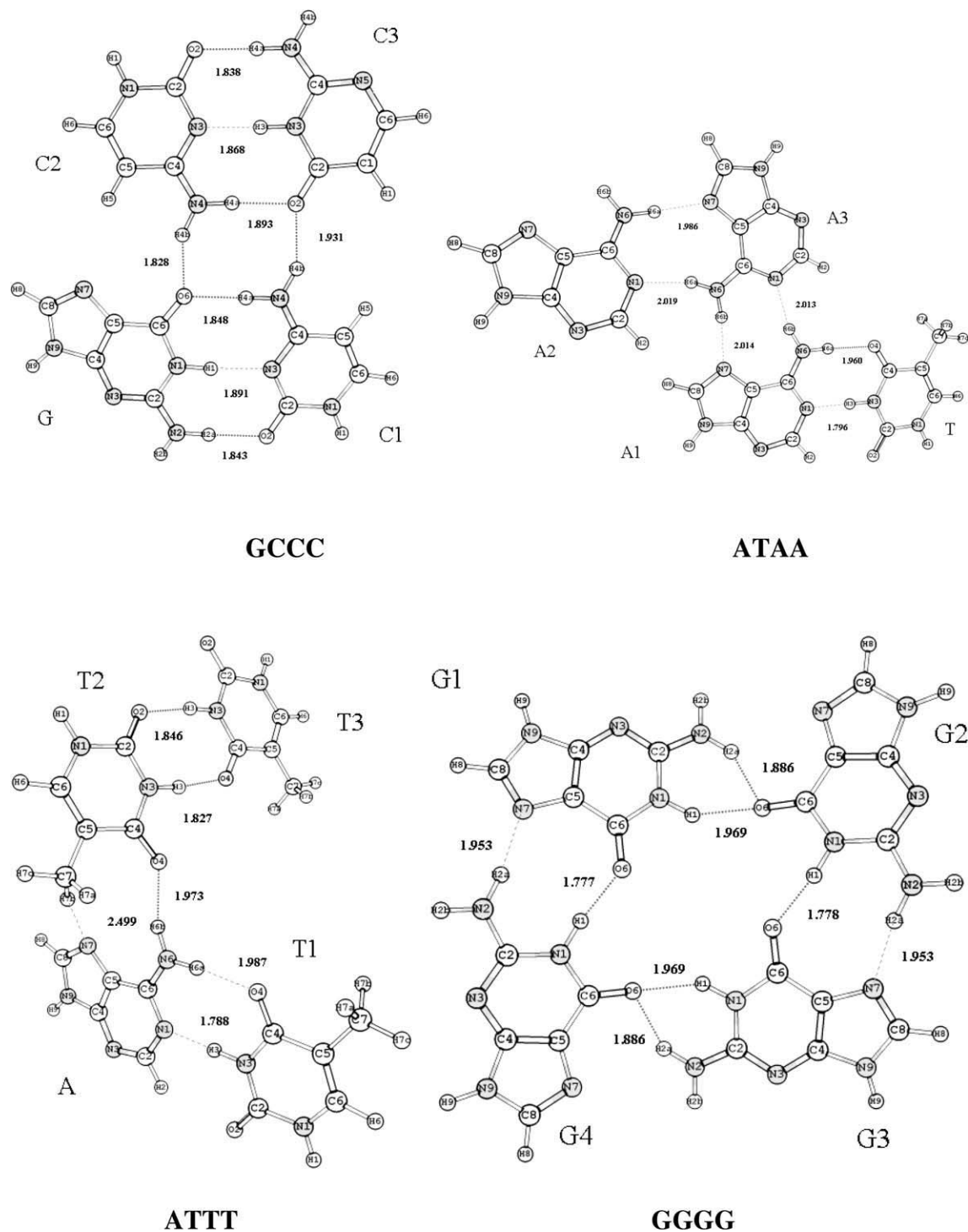


FIGURE 1. Continued.

From the Table II, it has been observed that the calculated interaction energies do reflect the influence of structural changes induced by interaction of bases and inhibitor within the tetrads. In the

2,6-diaminoanthraquinone interacting tetrads, GCGC-ANTH is having more interaction energy of -83.16 kcal/mol and ATAT-ANTH has possesses less interaction energy of -31.59 kcal/mol.

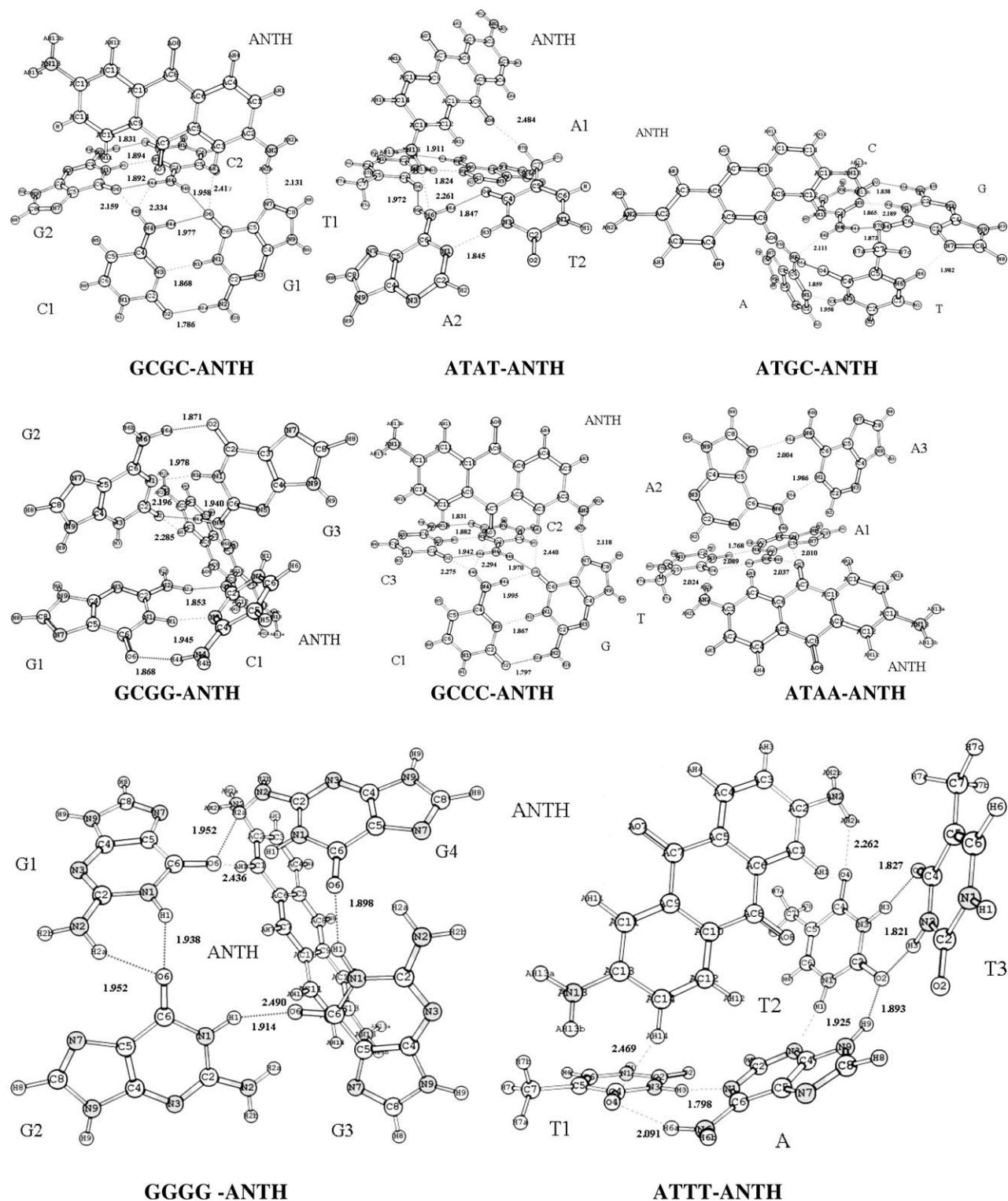


FIGURE 2. The structures of 2,6 diaminoanthraquinone interacting complexes (GCGC-ANTH, ATAT-ANTH, ATGC-ANTH, GCGG-ANTH, GCCC-ANTH, ATAA-ANTH, GGGG-ANTH, and ATTT-ANTH) optimized at B3LYP/6-31G** level of theory (IUPAC number has been followed for labeling of atoms and for inhibitor "A" has been added along with the atom number).

TABLE I

Hydrogen bond length H...Y (in Å), electron density ρ (in au), Laplacian of electron density $\nabla^2\rho$ (in au), and the hydrogen bond stabilization energy E^2 (in kcal/mol) correspond to hydrogen bonds in inhibitor interacting complexes.

	H...Y	ρ	$\nabla^2\rho$	E^2		H...Y	ρ	$\nabla^2\rho$	E^2
ATAA-ANTH					ATAT-ANTH				
N3-H3...N1	1.768	0.047	0.098	34.04	N6-H6a...O4	1.846	0.033	0.093	12.75
N6-H6a...O4	2.089	0.019	0.051	4.72	N3-H3...N1	1.844	0.039	0.088	26.45
AN2-AH2a...O4	2.024	0.021	0.061	6.06	AN13-AH13a...N6	2.258	0.016	0.039	5.7
N6-H6b...AO7	2.037	0.02	0.059	4.26	AC8-AO8...H7a	2.481	0.008	0.029	1.07
N6-H6b...AO7	2.010	0.021	0.063	5.26	N6-H6a...O2	1.909	0.028	0.078	9.58
N6-H6a...N1	1.986	0.029	0.069	15.75	N3-H3...N1	1.824	0.041	0.089	28.85
N6-H6a...N7	2.004	0.027	0.065	15.56	—	—	—	—	—
ATTT-ANTH					ATGC-ANTH				
N3-H3...O4	1.827	0.033	0.097	12.93	N4-H4a...O6	1.838	0.033	0.092	13.72
N3-H3...O2	1.821	0.034	0.096	10.06	N1-H1...N2	1.865	0.037	0.084	25.18
N1-H1...N3	1.925	0.032	0.075	18.77	N2-H2a...O2	1.873	0.030	0.086	9.84
N9-H9...O2	1.893	0.029	0.082	4.42	N4-H4b...N6	2.111	0.022	0.051	9.89
N3-H3...N1	1.798	0.043	0.095	29.37	N6-H6a...O4	1.859	0.032	0.088	9.32
N6-H6a...O4	2.09	0.019	0.052	5.39	N3-H3...N1	1.958	0.030	0.073	17.33
AN1-AH13b...O4	2.262	0.013	0.041	1.93	AN13-AH13a...O6	2.189	0.016	0.045	1.74
GGGG-ANTH					GCGG-ANTH				
N1-H1...O6	1.937	0.025	0.079	8.22	N4-H4a...O6	1.868	0.031	0.087	10.56
N2-H2a...O6	1.954	0.028	0.076	8.82	N1-H1...N3	1.945	0.031	0.074	17.41
N1-H1...O6	1.914	0.026	0.084	9.61	N2-H2a...O2	1.853	0.032	0.091	8.85
N2-H2a...O6	1.994	0.025	0.068	8.07	N9-H9...N9	2.435	0.011	0.029	2.43
N1-H1...O6	1.900	0.027	0.086	9.32	N5-H5...N2	2.008	0.027	0.065	9.02
AN2-AH2a...N7	2.199	0.018	0.045	7.85	N2-H2b...O2	2.054	0.021	0.062	4.12
N2-H2a...O6	1.949	0.027	0.075	7.81	N1-H1...N3	2.025	0.026	0.062	10.74
N1-H1...O6	2.023	0.020	0.066	6.71	AN2-AH2...O6	2.196	0.015	0.044	1.78
—	—	—	—	—	N2-H2a...O6	1.940	0.027	0.072	4.59
GCCC-ANTH					GCGC-ANTH				
N2-H2a...O2	1.797	0.036	0.103	16.18	N2-H2a...O2	1.831	0.034	0.094	14.49
N1-H1...N3	1.867	0.037	0.083	24.58	N1-H1...N3	1.894	0.035	0.079	23.14
N4-H4a...O6	1.995	0.024	0.066	6.6	N4-H4a...O6	1.892	0.029	0.081	10.36
N4-H4b...O6	1.970	0.023	0.068	6.93	N4-H4b...O6	2.158	0.024	0.071	6.98
N4-H4b...O2	2.57	0.012	0.046	2.64	AN2-AH2a...AN7	2.131	0.021	0.051	8.92
AN2-AH2a...N7	2.118	0.021	0.053	9.45	AC1-AH1...O6	1.958	0.010	0.031	1.38
N4-H4a...O2	2.2	0.027	0.070	9.82	N4-H4a...O6	1.977	0.025	0.068	6.92
N4-H4a...O2	1.831	0.034	0.094	14.52	N1-H1...N3	1.868	0.037	0.083	24.88
N20-H36...O65	2.294	0.012	0.050	1.51	N2-H2a...O2	1.786	0.037	0.106	17.11
AC3-AH3...O6	2.44	0.009	0.03	1.36	—	—	—	—	—

The interaction energy order is GCGC-ANTH > GGGG-ANTH > GCCC-ANTH > GCGG-ANTH > ATGC-ANTH > ATTT-ANTH > ATAA-ANTH > ATAT-ANTH. Molecular modeling studies [60–63] reveals that the tricyclic structure of anthraquinone interacts with the terminal guanine-quartet of DNA sequences and the interaction between substitutions of anthraquinone and DNA grooves further stabilize the complexes. Similarly, in the present study, the interaction of 2,6-diaminoanthraquinone with the DNA grooves stabilizes the

tetrads. The interaction of 2,6-diaminoanthraquinone with ATTT tetrad increases the interaction between the nucleobases, and hence, the interaction energy of ATTT-ANTH increases by –19 kcal/mol. In ATAT tetrad, though the inhibitor increases the interaction energy around 2 kcal/mol, the stability of the complex is found to be less as comparing with the other complexes. Further, the bending of nucleobases decreases the energy gain from extra hydrogen bond and decreases the stability of the ATAT-ANTH

TABLE II

Interaction energies ΔE (in kcal/mol) of 2,6-diaminoanthraquinone interacting complexes and their respective isolated tetrads calculated at B3LYP/6-31G** level of theory.

Base Pair	ΔE	Base Pair	ΔE	Base Pair	ΔE	Base Pair	ΔE
ATGC-ANTH		GCGC-ANTH		ATAT-ANTH		GCGG-ANTH	
$\Delta^2 E_{\text{iso}}$	-57.67	$\Delta^2 E_{\text{iso}}$	-81.14	$\Delta^2 E_{\text{iso}}$	-31.59	$\Delta^2 E_{\text{iso}}$	-72.39
ΔE_{Tot}	-62.23	ΔE_{Tot}	-83.16	ΔE_{Tot}	-33.61	ΔE_{Tot}	-76.02
$\Delta^2 E_{\text{com}}^{\text{(G+ANTH)}}$	-3.2	$\Delta^2 E_{\text{com}}^{\text{(G1+ANTH)}}$	2.49	$\Delta^2 E_{\text{com}}^{\text{(A1+ANTH)}}$	-1.74	$\Delta^2 E_{\text{com}}^{\text{(G1+ANTH)}}$	-3.97
$\Delta^2 E_{\text{com}}^{\text{(C+ANTH)}}$	-0.72	$\Delta^2 E_{\text{com}}^{\text{(G2+ANTH)}}$	-4.86	$\Delta^2 E_{\text{com}}^{\text{(A2+ANTH)}}$	1.03	$\Delta^2 E_{\text{com}}^{\text{(G2+ANTH)}}$	-1.28
$\Delta^2 E_{\text{com}}^{\text{(A+ANTH)}}$	-0.39	$\Delta^2 E_{\text{com}}^{\text{(C1+ANTH)}}$	-0.87	$\Delta^2 E_{\text{com}}^{\text{(T1+ANTH)}}$	-1.85	$\Delta^2 E_{\text{com}}^{\text{(G3+ANTH)}}$	-5.66
$\Delta^2 E_{\text{com}}^{\text{(T+ANTH)}}$	0.18	$\Delta^2 E_{\text{com}}^{\text{(C2+ANTH)}}$	-3.83	$\Delta^2 E_{\text{com}}^{\text{(T2+ANTH)}}$	-0.95	$\Delta^2 E_{\text{com}}^{\text{(C+ANTH)}}$	3.56
$\Delta^2 E_{\text{GC}}$	-29.2	$\Delta^2 E_{\text{G1C1}}$	-29.51	$\Delta^2 E_{\text{A1T1}}$	-13.14	$\Delta^2 E_{\text{G1C}}$	-24.55
$\Delta^2 E_{\text{AT}}$	-10.87	$\Delta^2 E_{\text{G2C2}}$	-28.56	$\Delta^2 E_{\text{A2T2}}$	-13.54	$\Delta^2 E_{\text{G2G3}}$	-24.55
$\Delta^2 E_{\text{CT}}$	-1.29	$\Delta^2 E_{\text{G1G2}}$	0.82	$\Delta^2 E_{\text{A1A2}}$	-0.089	$\Delta^2 E_{\text{G1G2}}$	2.97
$\Delta^2 E_{\text{AC}}$	-3.29	$\Delta^2 E_{\text{G1C2}}$	-6.94	$\Delta^2 E_{\text{A1T2}}$	-4.63	$\Delta^2 E_{\text{G1G3}}$	-9.9
$\Delta^2 E_{\text{AG}}$	0.075	$\Delta^2 E_{\text{G2C1}}$	-8.34	$\Delta^2 E_{\text{A2T1}}$	-0.49	$\Delta^2 E_{\text{G2C}}$	-12.02
$\Delta^2 E_{\text{GT}}$	-10.56	$\Delta^2 E_{\text{C1C2}}$	-2.02	$\Delta^2 E_{\text{T1T2}}$	1.36	$\Delta^2 E_{\text{G3C}}$	-1.53
$\Delta^5 E$	-2.9	$\Delta^5 E$	1.54	$\Delta^5 E$	0.43	$\Delta^5 E$	0.91
GCCC-ANTH		ATAA-ANTH		ATTT-ANTH		GGGG-ANTH	
$\Delta^2 E_{\text{iso}}$	-78.77	$\Delta^2 E_{\text{iso}}$	-35.41	$\Delta^2 E_{\text{iso}}$	-29.68	$\Delta^2 E_{\text{iso}}$	-78.59
ΔE_{Tot}	-80.43	ΔE_{Tot}	-35.19	ΔE_{Tot}	-48.37	ΔE_{Tot}	-81.72
$\Delta^2 E_{\text{com}}^{\text{(G+ANTH)}}$	-5.04	$\Delta^2 E_{\text{com}}^{\text{(A1+ANTH)}}$	-2.16	$\Delta^2 E_{\text{com}}^{\text{(A+ANTH)}}$	1.19	$\Delta^2 E_{\text{com}}^{\text{(G1+ANTH)}}$	-4.26
$\Delta^2 E_{\text{com}}^{\text{(C1+ANTH)}}$	-4.03	$\Delta^2 E_{\text{com}}^{\text{(T+ANTH)}}$	-4.18	$\Delta^2 E_{\text{com}}^{\text{(T1+ANTH)}}$	-2.54	$\Delta^2 E_{\text{com}}^{\text{(G2+ANTH)}}$	0.20
$\Delta^2 E_{\text{com}}^{\text{(C2+ANTH)}}$	-0.93	$\Delta^2 E_{\text{com}}^{\text{(A2+ANTH)}}$	-4.99	$\Delta^2 E_{\text{com}}^{\text{(T2+ANTH)}}$	-3.37	$\Delta^2 E_{\text{com}}^{\text{(G3+ANTH)}}$	-0.69
$\Delta^2 E_{\text{com}}^{\text{(C3+ANTH)}}$	2.2	$\Delta^2 E_{\text{com}}^{\text{(A3+ANTH)}}$	-0.44	$\Delta^2 E_{\text{com}}^{\text{(T3+ANTH)}}$	-2.18	$\Delta^2 E_{\text{com}}^{\text{(G4+ANTH)}}$	-1.49
$\Delta^2 E_{\text{GC1}}$	-28.05	$\Delta^2 E_{\text{A1T}}$	-0.02	$\Delta^2 E_{\text{AT1}}$	-12.57	$\Delta^2 E_{\text{G1G2}}$	-14.21
$\Delta^2 E_{\text{C2C3}}$	-29.36	$\Delta^2 E_{\text{A2A3}}$	-11.49	$\Delta^2 E_{\text{T2T3}}$	-10.39	$\Delta^2 E_{\text{G1G3}}$	-14.48
$\Delta^2 E_{\text{GC2}}$	-8.2	$\Delta^2 E_{\text{A1A2}}$	-0.15	$\Delta^2 E_{\text{AT2}}$	-16.87	$\Delta^2 E_{\text{G1G4}}$	-1.79
$\Delta^2 E_{\text{GC3}}$	0.55	$\Delta^2 E_{\text{A1A3}}$	0.47	$\Delta^2 E_{\text{AT3}}$	-1.14	$\Delta^2 E_{\text{G3G4}}$	-14.29
$\Delta^2 E_{\text{C1C2}}$	2.4	$\Delta^2 E_{\text{TA2}}$	1.05	$\Delta^2 E_{\text{T1T2}}$	-0.45	$\Delta^2 E_{\text{G2G3}}$	-1.70
$\Delta^2 E_{\text{C1C3}}$	-5.09	$\Delta^2 E_{\text{TA3}}$	0.15	$\Delta^2 E_{\text{T1T3}}$	0.05	$\Delta^2 E_{\text{G2G4}}$	-14.47
$\Delta^5 E$	-4.88	$\Delta^5 E$	-13.43	$\Delta^5 E$	-0.1	$\Delta^5 E$	-14.54

$\Delta^2 E_{\text{iso}}$ is the interaction energy of isolated tetrad, ΔE_{Tot} is the total interaction energy of complex, $\Delta^2 E_{\text{com}}^{\text{(G+ANTH)}}$ is the interaction energy of Guanine base with inhibitor and similarly for other bases, $\Delta^2 E_{\text{GG}}$ is the interaction energy of guanine bases without inhibitor and similarly for other bases and $\Delta^5 E$ is the many body interaction energy.

complex. The distortions induced by the inhibitor around amine, keto, and amide bonds may reduce π -electron conjugation within the bases and destabilize the tetrads.

It has been observed that the guanine and cytosine based tetrads are more stable than adenine and thymine based tetrads. Gavathiotis et al. [14] have reported that the DNA sequences with adenine nucleotide are less stable than the sequences with guanine base because only half of the surface area of the adenine tetrad is involved in stacking interactions. The above results are reflected in the calculated electron density and Laplacian of electron density values listed in Table I, where the strong hydrogen bonds are found to be associated with higher electron density and

higher Laplacian of electron density at bond critical points, indicating the stability of the complexes.

As explained earlier, the active sites such as carbonyl and amino groups of the inhibitor mainly bind at the edges of the DNA grooves, which lead to minimum interaction with the inter-acted nucleobases. The many body interaction energy analysis shows that for few cases the energy corresponding to the interaction between the inhibitor and nucleobases is positive. For example, T-ANTH, G-ANTH, A2-ANTH, C-ANTH, A-ANTH, G2-ANTH in ATGC-ANTH, GCGC-ANTH, ATAT-ANTH, GCGG-ANTH, GCCC-ANTH, ATTT-ANTH, GCGC-ANTH, respectively (see Table II). In few ANTH interacting

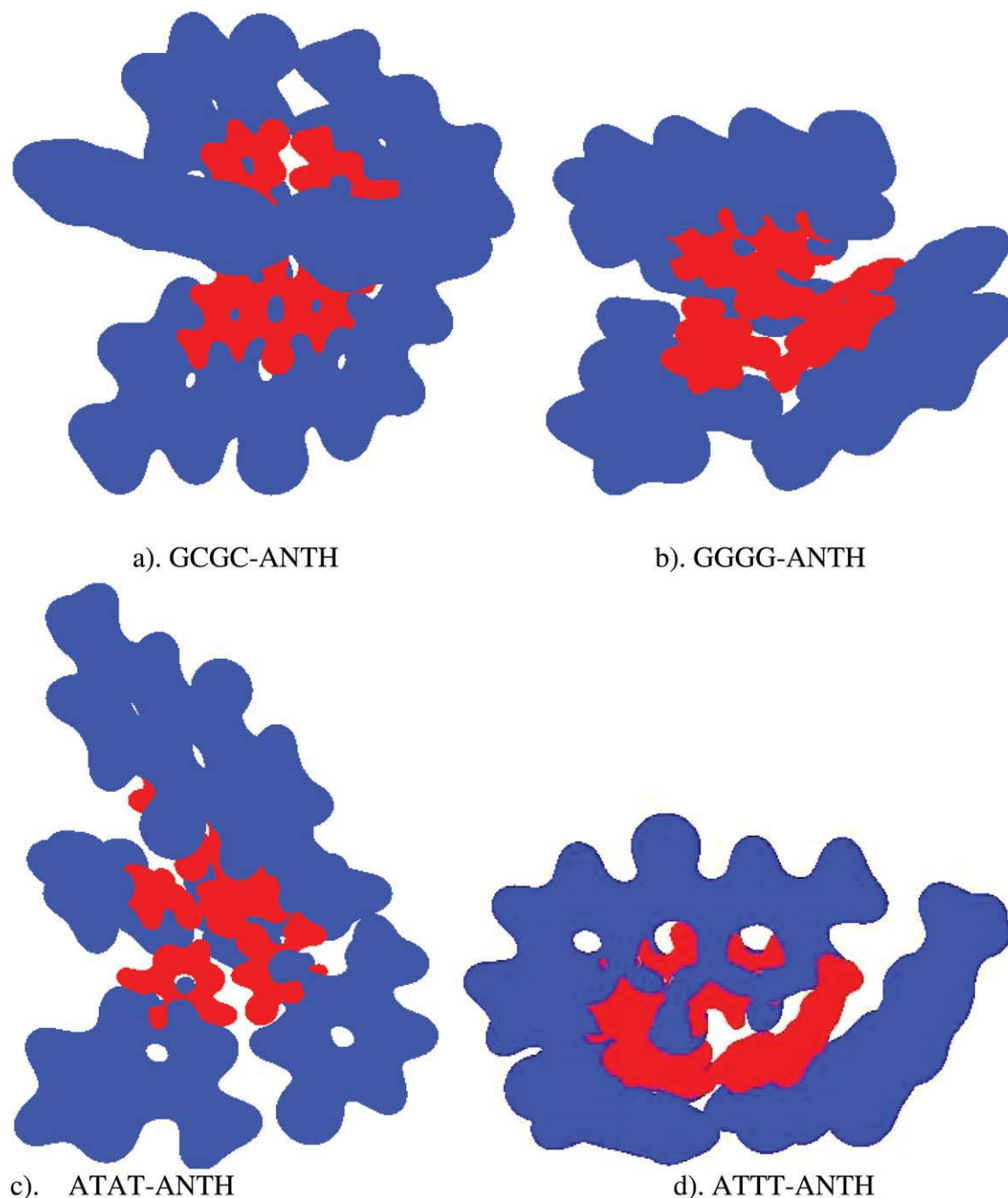


FIGURE 3. Electron density difference maps for most inhibitor interacting complexes (a) GCGC-ANTH, (b) GGGG-ANTH and least inhibitor interacting complexes, (c) ATAT-ANTH, and (d) ATTT-ANTH. Here, blue regions represent the gain in electron density as a result of formation of the inhibitor interacting complex relative to noninteracting nucleobases and inhibitor molecule; red regions refer to loss of electron density. The contour shown is 0.05 e/au^3 . [Color figure can be viewed in the online issue, which is available at wileyonlinelibrary.com.]

tetrads, the positive interaction energy has been observed between two bases. Although the interaction between GG bases in GCGC-ANTH is positive, the strong interaction between GC base

pairs and nucleobases with inhibitor makes the complex to remain stable with interaction energy of -83.16 kcal/mol . For less stable 2,6-diaminoanthraquinone interacting complexes, the

many body interaction energy is found to be positive.

The electron density difference map has been plotted for the complexes GCGC-ANTH, GGGG-ANTH, ATAT-ANTH, and ATTT-ANTH. Hydrogen bond can be characterized as the transfer of electron density between the interacting orbitals. The electron density difference maps as shown in Figure 3 provide the information about gain or loss of electron density within the interacting molecules. In the complexes GCGC-ANTH and GGGG-ANTH, the maximum amount of electron density is gained at the proton acceptor region and less amount of electron density is lost at the proton donor moiety. For the complexes ATAT-ANTH and ATTT-ANTH, a comparatively less amount of electron density is gained and lost by their respective proton acceptors and donors. The total energy and dipole moment of the isolated tetrads and inhibitor interacting tetrads in the gas and aqueous phases ($\epsilon = 78.5$) were calculated at B3LYP/6-31G** level of theory and dipole moment values are given in Figure 4. The total energy reveals that the solvent interaction with the molecular system has increased the stability of the isolated tetrads and complexes. The stability order is found to be same in the gas and aqueous phases. Figure 4 shows that irrespective of the medium, the dipole moment calculated for GGGG tetrad is found to be large and GCGC tetrad is having low dipole moment value.

The electron density ρ , Laplacian of electron density $\nabla^2\rho$, and the hydrogen bond stabilization energy E^2 calculated by AIM and NBO analysis have been summarized in Table II. The stabilization energy E^2 corresponding to hydrogen bond interactions can be considered as the total charge transfer energy. There is an exponential correlation between the hydrogen bond length and stabilization energy E^2 , which indicates a rapid fall of stabilization energy with increase in hydrogen bond length. For the cases in which proton acceptor interacts with two proton donor, the stabilization energy is smaller in comparison with other hydrogen bonds and also C—H...O interactions have less stabilization energies as shown in Table I, which is reflected in the calculated electron density values. The electron density and Laplacian of electron density calculated for C—H...O type hydrogen bonds are found to be very small, while comparing the above values with N—H...N and N—H...O type hydrogen bonds. As expected, the electron density and the Laplacian of electron

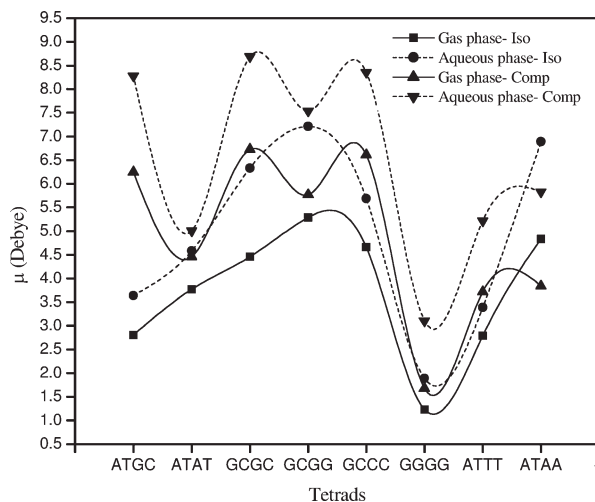


FIGURE 4. Dipole moment (in Debye) of isolated and ANTH interacting tetrads in gas and aqueous phases.

density are decreases as the hydrogen bond length increases. The electron density values calculated at the BCPs augment, the stability order predicted through the interaction energy. In general, the electron density and charge transfer analysis reveals the strong binding nature of 2,6-diaminoanthraquinone inhibitor with studied tetrads. It is expected that the ANTH is a suitable inhibitor for telomerase activity in DNA as demonstrated by NMR studies.

4. Conclusions

The nucleobases tetrads such as GGGG, GCGC, ATGC, ATAT, ATAA, ATTT, GCCC, GCGG, and their 2,6-diaminoanthraquinone interacting complexes have been studied using density functional theory method in gas and aqueous phases. It is found that the inhibitor binds strongly with the tetrads through hydrogen bond interaction and alters the geometry of the tetrads. Because of the formation of bifurcated hydrogen bonds in GCCC and GCGC tetrads, the structures were observed with planar or near planar structure. The presence of solvent increases the stability and dipole moment of the isolated tetrads and complexes. The presence of hydrogen bonds has been identified and studied through the interaction energy and many body interaction energy, topological, and NBO analysis. The interaction energy of isolated tetrads and complexes reveals that the guanine and cytosine based tetrads are more stable

than adenine and thymine based tetrads. In the inhibitor interacting complexes, the many body interaction energy values show that the two-body interactions are stronger than the many body interactions. The electron density difference maps illustrate the delocalization of the electron density in the inhibitor interacting complexes. The results obtained from interaction energy, electron density difference map, topological, and NBO charge transfer analysis reveals the strong binding nature of 2,6-diaminoanthraquinone with studied tetrads indicating that this inhibitor is suitable to stabilize the above tetrads and inhibit the telomerase activity. The above results confirm that 2,6-diaminoanthraquinone may be used as a novel potential anticancer agent.

ACKNOWLEDGMENTS

The authors are thankful to the DST (Department of Science and Technology), Government of India for establishing the Central Computer Lab under the DST-FIST program, where most of the calculations have been performed. Further the authors express their sincere thanks to HPFC (High Performance Computing Facility) of DST at Hyderabad for allowing us to use the facility for the same calculations. One of the authors P. Deepa expresses her sincere thanks to CSIR, New Delhi, for the award of Senior Research Fellowship.

References

- Arthanari, H.; Bolton, P. H. *Chem Biol* 2001, 8, 221.
- Shafer, R. H.; Smirnov, I. *Biopolymers* 2001, 56, 209.
- Neidle, S.; Read, M. A. *Biopolymers* 2000–2001, 56, 195.
- Blackburn, E. H. *Cell* 1994, 77, 621.
- Zakian, V. A. *Science* 1995, 270, 1601.
- Bryan, T. M.; Cech, T. R. *Curr Opin Cell Biol* 1999, 11, 318.
- Harley, C. B.; Villeponteau, B. *Curr Opin Genet Dev* 1995, 5, 249.
- Allsopp, R. C.; Chang, E.; Kashefi-Azad, M.; Rogaev, E. I.; Piatyszek, M. A.; Shay, J. W.; Harley, C. B. *Exp Cell Res* 1995, 220, 194.
- Ulaner, G. A.; Hu, J. F.; Vu, T. H.; Giudice, L. C.; Hoffman, A. R. *Cancer Res* 1998, 58, 4168.
- Meyerson, M. *Toxicol Lett* 1998, 102–103, 41.
- (a) Neidle, S.; Kelland, L. R. *Anticancer Drug Des* 1999, 14, 341; (b) Neidle, S. *Curr Opin Struct Biol* 2009, 19, 239.
- Huang, H. S.; Chen, I. B.; Huang, K. F.; Lu, W. C.; Shieh, F. Y.; Huang, Y. Y.; Huang, F. C.; Lin, J. *J Chem Pharm Bull* 2007, 55, 284.
- Feng, J.; Funk, W. D.; Wang, S. S.; Weinrich, S. L.; Avilion, A. A.; Chiu, C. P.; Adams, R. R.; Chang, E.; Allsopp, R. C.; Yu, J.; Le, S.; West, M. D.; Harley, C. B.; Andrew, W. H.; Greider, C. W.; Villeponteau, B. *Science* 1995, 269, 1236.
- Gavathiotis, E.; Heald, R. A.; Stevens, M. F. G.; Searle, M. S. *Mol Biol* 2003, 334, 25.
- Perry, P. J.; Read, M. A.; Davies, R. T.; Gowan, S. M.; Reszka, A. P.; Wood, A. A.; Kelland, L. R.; Neidle, S. *J Med Chem* 1999, 42, 2679.
- Agbandje, M.; Jenkins, T. C.; McKenna, R.; Reszka, A. P.; Neidle, S. *J Med Chem* 1992, 35, 1418.
- Cairns, D.; Michalitsi, E.; Jenkins, T. C.; Mackay, S. P. *Bioorg Med Chem* 2002, 10, 803.
- Palumbo, M.; Palu, G.; Gia, O.; Ferrazzi, E.; Gastaldi, S.; Antonello, C.; Meloni, G. A. *Anticancer Drug Des* 1987, 1, 337.
- Collier, D. A.; Neidle, S. *J Med Chem* 1988, 31, 847.
- Keppeler, M. D.; Read, M. A.; Perry, P. J.; Trent, J. O.; Jenkins, T. C.; Reszka, A. P.; Neidle, S.; Fox, K. R. *Eur J Biochem* 1999, 263, 817.
- Li, N.; Ma, Y.; Yang, C.; Guo, L.; Yang, X. *Biophys Chem* 2005, 116, 199.
- Clark, G. R.; Pytel, P. D.; Squire, C. J.; Neidle, S. *J Am Chem Soc* 2003, 125, 4066.
- Louit, G.; Hocquet, A.; Ghomi, M.; Meyer, M.; Suhnel, J. *Phys Chem Commun* 2003, 6, 1.
- Liu, H.; Matsugami, A.; Katahira, M.; Uesugi, S. *J Mol Biol* 2002, 322, 955.
- Laughlan, G.; Murchie, A. I. H.; Norman, D. G.; Moore, M. P.; Moody, P. C. E.; Lilley, D. M. J.; Luisi, B. *Science* 1994, 265, 520.
- Phillips, K.; Dauter, Z.; Murchie, A. I. H.; Lilley, D. M. J.; Luisi, B. *J Mol Biol* 1997, 273, 171.
- Kang, C.; Zhang, X.; Moyzis, R.; Rich, A. *Nature* 1992, 356, 126.
- Bouaziz, S.; Kettani, A.; Patel, D. J. *J Mol Biol* 1998, 282, 637.
- Metzger, S.; Lippert, B. *J Am Chem Soc* 1996, 118, 12467.
- Kettani, A.; Kumar, R. A.; Patel, D. J. *J Mol Biol* 1995, 254, 638.
- Darlow, J. M.; Leach, D. R. F. *J Mol Biol* 1998, 275, 3.
- Kettani, A.; Bouaziz, S.; Gorin, A.; Zhao, H.; Jones, R. A.; Patel, D. J. *J Mol Biol* 1998, 282, 619.
- Leonard, G. A.; Zhang, S.; Peterson, M. R.; Harrop, S. J.; Helliwell, J. R.; Cruse, W. B. T.; Langlois, D.; Estaintot, B.; Kennard, O.; Grown, T.; Hunter, W. N. *Structure* 1995, 3, 335.
- Gu, J.; Leszczynski, J. *J Phys Chem A* 2000, 104, 7353.
- Gu, J.; Leszczynski, J. *J Phys Chem A* 2000, 104, 1898.
- Gu, J.; Wang, J.; Leszczynski, J. *J Phys Chem B* 2004, 108, 9277.
- Sun, W.; Hattman, S.; Kool, E. *J Mol Biol* 1997, 273, 765.
- Deepa, P.; Kolandaivel, P. *J Biol Struct Dyn* 2008, 25, 1.
- Becke, A. D. *Phys Rev A* 1988, 38, 3098.
- Lee, C.; Yang, W.; Parr, R. G. *Phys Rev B* 1988, 37, 785.
- Miertus, S.; Scrocco, E.; Tomasi, J. *J Chem Phys* 1981, 55, 117.

42. Boys, S. F.; Bernardi, F. *Mol Phys* 1970, 19, 553.
43. Xantheas, S. S. *J Chem Phys* 1996, 104, 8821.
44. Bader, R. F. W. *Atoms in Molecules, A Quantum Theory*; Oxford Science Publications, Clarendon Press: London, 1990.
45. Popelier, P. L. A.; Bader, R. F. W. *Chem Phys Lett* 1992, 189, 542.
46. Cheeseman, J. R.; Carroll, M. T.; Bader, R. F. W. *Chem Phys Lett* 1988, 143, 450.
47. Koch, U.; Popelier, P. L. A. *J Phys Chem* 1995, 99, 9747.
48. Gledening, E. D.; Reed, A. E.; Carpenter, J. A.; Weinhold, F. *NBO Version 3.1, Late-1980s Vintage*.
49. Frisch, M. J.; Trucks, G. W.; Schlegel, H. B.; Scuseria, G. E.; Robb, M. A.; Cheeseman, J. R.; Zakrzewski, V. G.; Montgomery, J. A.; Stratmann, R. E., Jr.; Burant, J. C.; Dapprich, S.; Millam, J. M.; Daniels, A. D.; Kudin, K. N.; Strain, M. C.; Farkas, O.; Tomasi, J.; Barone, V.; Cossi, M.; Cammi, R.; Mennucci, B.; Pomelli, C.; Adamo, C.; Clifford, S.; Ochterski, J.; Petersson, G. A.; Ayala, P. Y.; Cui, Q.; Morokuma, K.; Malick, D. K.; Rabuck, A. D.; Raghavachari, K.; Foresman, J. B.; Cioslowski, J.; Ortiz, J. V.; Baboul, A. G.; Stefanov, B. B.; Liu, G.; Liashenko, A.; Piskorz, P.; Komaromi, I.; Gomperts, R.; Martin, R. L.; Fox, D. J.; Keith, T.; Al-Laham, M. A.; Peng, C. Y.; Nanayakkara, A.; Gonzales, C.; Challacombe, M.; Gill, P. M. W.; Johnson, B.; Chen, W.; Wong, M. W.; Andres, J. L.; Gonzalez, C.; Head-Gordon, M.; Replogle, E. S.; Pople, J. A. *Gaussian 03. Revision A.11.2*; Gaussian, Inc.: Pittsburgh, PA, 2005.
50. Gu, J.; Leszczynski, J.; Bansal, M. *Chem Phys Lett* 1999, 311, 209.
51. Meyer, M.; Brandl, M.; Suhnel, J. *J Phys Chem A* 2001, 105, 8223.
52. Petraccone, L.; Erra, E.; Esposito, V.; Randazzo, A.; Mayol, L.; Nasti, L.; Barone, G.; Giancola, C. *Biochemistry* 2004, 43, 4877.
53. Meyer, M.; Schneider, C.; Brandl, M.; Suhnel, J. *J Phys Chem A* 2001, 105, 11560.
54. Parkinson, G. N.; Lee, M. P. H.; Neidle, S. *Nature* 2002, 417, 876.
55. Seela, F.; Kroschel, R. *Bioconjugate Chem* 2001, 12, 1043.
56. Gu, J.; Leszczynski, J. *J Phys Chem A* 2002, 106, 529.
57. Gu, J.; Leszczynski, J. *J Phys Chem A* 2001, 105, 10366.
58. Sponer, J.; Mokdad, A.; Sponer, J. E.; Spackova, N.; Leszczynski, J.; Leontis, N. *J Mol Biol* 2003, 330, 967.
59. Hobza, P.; Sponer, J. *Chem Rev* 1999, 99, 3247.
60. Sun, B.; Thompson, B. E.; Cathers, M.; Salazar, S.; Kerwin, M.; Trent, J. O.; Jenkins, T. C.; Neidle, S.; Hurley, L. H. *J Med Chem* 1997, 40, 2113.
61. Anantha, N. V.; Azam, M.; Sheardy, N. R. D. *Biochemistry* 1998, 37, 2709.
62. Hurley, L. H.; Wheelhouse, R. T.; Sun, D.; Kerwin, S. M.; Salazar, M.; Fedoroff, O. Y.; Han, F. X.; Han, H.; Izbicka, E.; Von Hoff, D. D. *Pharmacol Ther* 2000, 85, 141.
63. Neidle, S.; Parkinson, G. *Nat Rev Drug Discov* 2002, 1, 383.